

A non-intrusive stochastic Galerkin approach for modeling uncertainty propagation in deformation processes

Swagato Acharjee, Nicholas Zabaras¹

*Materials Process Design and Control Laboratory, Sibley School of Mechanical and
Aerospace Engineering, 188 Frank H.T. Rhodes Hall, Cornell University, Ithaca,
NY 14853-3801, USA*

Abstract

Large Deformation processes are inherently complex involving complicated phenomena and high degrees of non-linearity. Stochastic analysis of these processes is a formidable task considering the numerous sources of uncertainties and random parameters that may influence the process. As a result, uncertainty propagation using intrusive techniques, though achieved in the past, may require tortuous analysis, overhaul of the internal structure of existing deterministic softwares or significant additions. In this paper we present an approach called Non-Intrusive Stochastic Galerkin (NISG) method, which can be directly applied to presently available deterministic softwares with minimal effort for computing the complete PDF of the stochastic process. The method involves finite element discretization of the random support space and piecewise continuous interpolation of the PDF over the support space with deterministic function evaluations at the element integration points. For the hyperelastic-viscoplastic large deformation problems considered here with varying levels of randomness in the input and boundary conditions, the NISG method provides highly accurate estimates of the statistical quantities of interest within a fraction of the time required using existing monte-carlo methods.

1 Introduction

Modeling and simulation of large inelastic deformations processes is extremely complex considering the nonlinear coupled phenomena that need to be ac-

¹ Corresponding author: Fax: 607-255-1222
Email: zabaras@cornell.edu
URL: <http://mpdc.mae.cornell.edu/>

counted for. These involve large deformation plasticity, microstructure evolution, non-linear contact and friction conditions, thermal effects and damage accumulation. It is well known that all these phenomena are inherently statistical in nature and are a source of randomness in the process. Uncertainties also creep in from various process parameters, initial and boundary conditions. Although there has been substantial progress made in the modeling and simulation of these processes, almost all of it has been in the deterministic domain.

Considering their complexity, a Monte-Carlo based stochastic analysis of deformation process although relatively non-intrusive and trivial to implement is prohibitively expensive due to the large number of samples required. As a result they can only be used as a verification tool for comparing with other efficient techniques. Some attempts have been made in the past for stochastic analysis of these processes. Taylor series based methods were applied to metal forming and inelastic deformation processes in [1]-[4]. These methods, which also include reliability analysis using (FORM/SORM) are crude approximations which require less computations and are suitable for small levels of uncertainties. Up to second order statistics can be computed using these techniques with relative ease. Computing statistics of higher orders, though not impossible, becomes difficult due to the complex nature of the underlying mathematical descriptions. A regression based response surface method was employed in [5]. A Lagrangian description of finite deformation processes using polynomial chaos expansions [6] was presented in [7]. Applications involving uncertainties in geometry, material properties, initial and boundary conditions were presented. Though the method gives accurate description of the randomness even for large levels of input uncertainty, it requires operations on spectral expansions of the random variables and is thus difficult to implement. Also the method fails when there are functions with steep gradients and steps in the random behavior of the system, since spectral expansion of such functions can never be approximated efficiently using polynomial expansions.

In this paper, our efforts are concentrated specifically in developing a robust non-intrusive stochastic analysis method for inelastic deformation processes which provide full statistics of the uncertainties in the output consisting of the PDF and higher order moments and not just a few statistical parameters. Not only are these methods faster than monte-carlo simulations, they also require minimal implementation effort compared to the intrusive methods. Hence they are very well-suited for coupling with existing simulation codes without any significant work. As a result, they provide a practical approach for probabilistic analysis of highly complex processes which have already been analysed in the deterministic domain using established and verified computer codes.

Some earlier versions of non-intrusive methods have been applied in the past to explain stochastic phenomena in varied areas. Tatang et al. [8] developed a Polynomial Chaos based spectral collocation approach which was applied to problems of direct radiative forcing in sulfate aerosols. Hussaini et al. [9] applied the spectral collocation method to analyze randomness in quasi 1-D nozzle flow. A Non Intrusive Spectral Projection technique for uncertainty

quantification in reacting-flow simulations was developed in [10] though it required costly monte carlo simulations. The method we apply is based on the Stochastic Galerkin approach [11] in which the random space is discretized using finite elements. The problem is solved deterministically at the integration points from which the statistics of the desired quantities can be obtained.

The plan of the paper is as follows. The next section provides a brief review of the updated Lagrangian approach for modeling hyperelastic-viscoplastic deformation processes. Details on polynomial representation of stochastic processes are presented in Section 3. Section 4 provides details of the proposed non-intrusive technique with extensions to reliability analysis as well as a discussion of an analogous intrusive approach. Numerical examples are presented in Section 5. Finally we conclude in Section 6.

2 Review of large deformation processes

A review of the Lagrangian FEM formulation for the hyperelastic-viscoplastic large deformation problem is presented next. The problem can be stated as follows: Compute the time history of the deformation, temperature, material state and plastic deformation of a body deforming as a result of external forces and/or deformation due to contact and friction at the workpiece-die interface.

The deformation problem is sub-divided into kinematic, constitutive, contact and thermal sub-problems. We follow an updated Lagrangian formulation to solve the direct deformation problem in a generic forming stage in which material occupying an initial configuration \mathbf{B}_0 is deformed to obtain a final configuration $\mathbf{B}_f(t = t_f)$. To compute the material configuration \mathbf{B}_{n+1} for $n = 0, 1, \dots, (f - 1)$, one proceeds in an incremental fashion using the configuration \mathbf{B}_n as the reference configuration. In this review, analysis of a single-stage process is provided with the details of multi-stage processes given in [12].

Let \mathbf{X} be a material particle in \mathbf{B}_0 and let $\mathbf{x} = \tilde{\mathbf{x}}(\mathbf{X}, t_{n+1})$ be its location at time t_{n+1} . The total deformation gradient can be defined as

$$\mathbf{F}(\mathbf{X}, t_{n+1}) = \nabla_0 \tilde{\mathbf{x}}(\mathbf{X}, t_{n+1}) = \frac{\partial \tilde{\mathbf{x}}(\mathbf{X}, t_{n+1})}{\partial \mathbf{X}} \quad (2.1)$$

In an appropriate kinematic framework for large deformation inelastic analysis including thermal effects, the total deformation gradient is decomposed into thermal, plastic and elastic parts as follows:

$$\mathbf{F} \equiv \mathbf{F}_{n+1} = \mathbf{F}^e \mathbf{F}^p \mathbf{F}^\tau \quad (2.2)$$

where \mathbf{F}^e is the elastic deformation gradient, \mathbf{F}^p , the plastic deformation gradient and \mathbf{F}^τ is the thermal part of the deformation gradient in \mathbf{B}_{n+1} .

Using an updated Lagrangian framework, the total deformation gradient \mathbf{F}_{n+1} at time $t = t_{n+1}$ can be expressed in terms of \mathbf{F}_n at time $t = t_n$ as follows:

$$\mathbf{F}_{n+1} = \mathbf{F}_r \mathbf{F}_n \quad (2.3)$$

where \mathbf{F}_r is the relative deformation gradient. In the absence of body forces, the equilibrium equation at $t = t_{n+1}$ can be expressed in the reference configuration \mathbf{B}_n as,

$$\nabla_n \cdot \mathbf{P}_r = 0 \quad (2.4)$$

where ∇_n denotes the divergence in \mathbf{B}_n . The Piola-Kirchhoff I stress \mathbf{P}_r is expressed per unit area of \mathbf{B}_n and given as follows:

$$\mathbf{P}_r = \det \mathbf{F}_r \mathbf{T} \mathbf{F}_r^{-T} \quad (2.5)$$

where \mathbf{T} is the Cauchy stress. For elastic deformations we employ a hyperelastic constitutive law given by:

$$\bar{\mathbf{T}} = \mathcal{L}^e[\bar{\mathbf{E}}^e] \quad (2.6)$$

where \mathcal{L}^e is the fourth order elasticity tensor. $\bar{\mathbf{T}}$ and $\bar{\mathbf{E}}^e$ are the conjugate strain and stress measures defined with respect to an unstressed intermediate configuration. The plastic flow is modelled using the classical state variable based J_2 flow theory. The evolution of \mathbf{F}^p is given by

$$\bar{\mathbf{L}}^p = \bar{\mathbf{D}}^p = \dot{\mathbf{F}}^p (\mathbf{F}^p)^{-1} = \sqrt{\frac{3}{2}} \frac{\dot{\bar{\mathbf{T}}}'}{\|\bar{\mathbf{T}}'\|} \quad (2.7)$$

where it is assumed that in the intermediate configuration $\bar{\mathbf{W}}^p = 0$. The evolution of the equivalent plastic strain $\tilde{\epsilon}^p$ is given by

$$\dot{\tilde{\epsilon}}^p = f(\tilde{\sigma}, s, \tau) \quad (2.8)$$

while the evolution of the state variable s is given by

$$\dot{s} = g(\tilde{\sigma}, s, \tau) \quad (2.9)$$

The constitutive problem is solved using a radial return type algorithm. The evolution of the thermal deformation gradient is given by:

$$\dot{\mathbf{F}}^\tau (\mathbf{F}^\tau)^{-1} = \beta \dot{\tau} \mathbf{I} \quad (2.10)$$

where \mathbf{I} is the identity tensor and β is the isotropic thermal expansion coefficient. The evolution of the workpiece temperature τ is obtained by solving a coupled thermal problem. The details are given in [13].

The solution of the deformation problem in the current processing stage proceeds incrementally in time starting from the initial configuration \mathbf{B}_0 . Each increment involves the solution of the virtual work equation given by:

$$\int_{\mathbf{B}_n} \mathbf{P}_r \cdot \nabla_n \tilde{\mathbf{u}} \cdot dV_n = \int_{\Gamma_n} \mathbf{t} \cdot \tilde{\mathbf{u}} dA_n \quad (2.11)$$

where the test displacement $\tilde{\mathbf{u}}$ is expressed over the initial configuration \mathbf{B}_n . The right hand side term in the above equation involves implicit traction conditions as a result of contact between surfaces. The contact problem is solved using an augmented Lagrangian framework detailed in [14].

The presented developments allow the use of any state variable-based constitutive model and can also be extended to evolution of ductile damage in materials. The details are given in our earlier work [14].

3 Polynomial representation of random processes

A real-valued function g having dependence on space (\mathbf{x}), time (t) and a random parameter (θ) with a known probability density function (PDF) is called a stochastic process and can be written as:

$$g(\mathbf{x}, t, \theta), \quad \mathbf{x} \in \mathcal{X}, t \in \mathcal{T}, \theta \in \Theta \quad (3.1)$$

The quantity Θ is called the support space of the random variable θ . To parametrize the support space in terms of the input random variables, we define a set of independent random variables $\{\xi_i\}_{i=1}^N$ spanning Θ . The joint PDF of these random variables can be represented as

$$f(\boldsymbol{\xi}) = \prod_{i=1}^N f_{\xi_i}(\xi_i) \quad (3.2)$$

The stochastic process is then represented as function of these independent random variables. Several forms of representation exist, which are briefly explained below.

3.1 Karhunen-Loève (KL) expansion:

The Karhunen-Loève (KL) expansion is based on the spectral expansion of a stochastic variable given its covariance kernel. For a stochastic process $g(\mathbf{x}, t, \boldsymbol{\xi})$ with a covariance kernel $\mathcal{R}(\mathbf{x}_1, t_1, \mathbf{x}_2, t_2)$ (where $\mathbf{x}_1, \mathbf{x}_2$ are spatial coordinates and t_1, t_2 are temporal coordinates), the truncated KL expansion is given by

$$g(\mathbf{x}, t, \boldsymbol{\xi}) = \bar{g}(\mathbf{x}, t) + \sum_{i=1}^N \sqrt{\lambda_i} \xi_i(\boldsymbol{\xi}) f_i(\mathbf{x}, t) \quad (3.3)$$

where $\bar{g}(\mathbf{x}, t)$ denotes the mean of the stochastic process and $\{\xi_i\}_{i=1}^N$ are a set of independent random variables spanning the probability space. The scalars λ_i and deterministic functions $f_i(\mathbf{x}, t)$ are the eigen-pairs of the covariance function, i.e.

$$\int \mathcal{R}(\mathbf{x}_1, t_1, \mathbf{x}_2, t_2) f_n(\mathbf{x}_1, t_1) d\mathbf{x} dt_1 = \lambda_n f_n(\mathbf{x}_2, t_2) \quad (3.4)$$

Of all possible expansions of a random process, the KL expansion is optimal in the mean square sense. However, its application is limited by the fact that the covariance function needs to be known a priori. This limitation is complemented by the use of another expansion technique known as the polynomial chaos expansion that is discussed next.

3.2 Generalized Polynomial Chaos expansion (GPCE):

The GPCE employs polynomials in multidimensional random variables as a trial basis for the probability space to represent a stochastic process. Consider a set of independent, identically distributed (iid) random variables denoted as $\{\xi_i\}_{i=0}^N$. A polynomial chaos representation of a random process can be written as:

$$\begin{aligned} g(\mathbf{x}, t, \boldsymbol{\xi}) = & a_0(\mathbf{x}, t) \Gamma_0 + \sum_{i_1=1}^{\infty} a_{i_1}(\mathbf{x}, t) \Gamma_1(\xi_{i_1}) \\ & + \sum_{i_1=1}^{\infty} \sum_{i_2=1}^{i_1} a_{i_1 i_2}(\mathbf{x}, t) \Gamma_2(\xi_{i_1}, \xi_{i_2}) + \dots \end{aligned} \quad (3.5)$$

where $\Gamma_p(\cdot)$ (popularly known as polynomial chaoses) are polynomials in (ξ_1, ξ_2, \dots) . The above equation can be re-written in a compact form as follows:

$$g(\mathbf{x}, t, \boldsymbol{\xi}) = \sum_{i=0}^{\infty} g_i(\mathbf{x}, t) \Phi_i \quad (3.6)$$

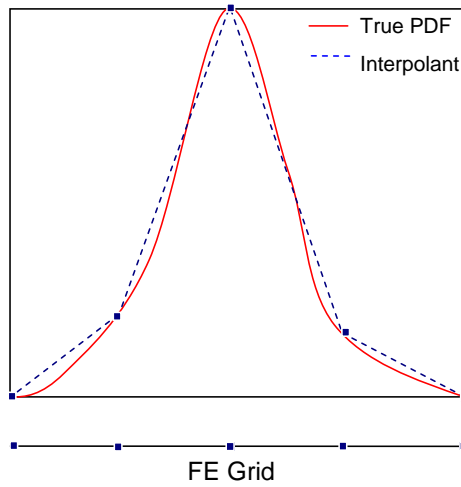


Fig. 1. Finite element discretization scheme for a one-dimensional PDF.

where there is one-to-one correspondence between the functionals $\Gamma_p(\bullet)$ and Φ_i . In actual practice, the random process is represented by a truncated chaos expansion with a limited number of terms.

3.3 Locally supported piecewise continuous representation:

In this method, the stochastic process is represented over the support space using piecewise continuous orthogonal polynomials in multi-dimensional random variables. The polynomials we choose are the locally supported element shape functions of a specific order used for representing functions in the finite element method. The space Θ spanned by these random variables is discretized using disjoint finite element subdomains leading to a new discretized space Θ^h where h is an element size parameter. This approximation can be denoted as

$$g(\mathbf{x}, t, \theta) = g(\mathbf{x}, t, \xi_1, \xi_2, \dots) \approx g^h(\mathbf{x}, t, \xi_1, \xi_2, \dots, \xi_N) = g^h(\mathbf{x}, t, \boldsymbol{\xi}).$$

Thus the stochastic process can be represented using the basis functions as

$$g^h(\mathbf{x}, t, \boldsymbol{\xi}) = \sum_{i=1}^{nodes} g_i^h \Phi_i \quad (3.7)$$

where Φ_i are the locally supported basis functions and g_i are the corresponding nodal values. A scheme for discretization of a one dimensional ($N = 1$) PDF is shown in Fig. 1.

Among the three representations discussed, the KLE leads to a global representation of the stochastic process over the random space. It is based on the eigen-decomposition of the covariance kernel which is a function of the spatial coordinates of the domain. Thus it is ideal for representing input uncertainties which may have a spatial variation such as material properties for which the

Covariance Kernel is known. The GPCE leads to a global polynomial type representation of the random function over the support space. Thus it is suitable for responses with smooth pdf's or responses devoid of any significant nonlinearities. It was shown in [15] and [16] that for functions involving high nonlinearities and critical points the GPCE fails to perform satisfactorily. On the other hand, a piecewise representation is ideally suited for representing discontinuities and nonlinearities in the processes. As mentioned before, finite deformation processes involve considerable degrees of nonlinearities at every stage. Thus we resort to the third approach - a piecewise representation using finite element basis functions for representation of the random large deformation processes in this work. This is also advantageous from a practical point of view since in converting a deterministic finite element based deterministic large deformation code to simulate stochastic deformation processes, these basis functions are available from other parts of the code and can be readily used for representing random functions.

4 Non-intrusive and intrusive approaches

The piecewise representation of the stochastic process which was discussed in the previous section, can lead to a non-intrusive decoupled as well as intrusive coupled formulation for evaluating the stochastic process. The two formulations are explained with an example of a solution of a linear system. We consider the evaluation of a random vector $u(\mathbf{x}, \boldsymbol{\xi})$ by the solution of a linear system which is defined by a random matrix $A(\boldsymbol{\xi})$ and a random vector $b(\boldsymbol{\xi})$ as shown below. (The superscript h has been dropped for notational simplicity)

$$A(\mathbf{x}, \boldsymbol{\xi})u(\mathbf{x}, \boldsymbol{\xi}) = b(\mathbf{x}, \boldsymbol{\xi}) \quad (4.1)$$

4.1 Intrusive coupled system

To solve the system using the coupled formulation, we first represent the above process in a N dimensional piecewise polynomial basis (equivalent to N nodes in the mesh)

$$A_i(\mathbf{x})\Phi_i(\boldsymbol{\xi})u_j(\mathbf{x})\Phi_j(\boldsymbol{\xi}) = b_k(\mathbf{x})\Phi_k(\boldsymbol{\xi}) \quad (4.2)$$

where $i, j, k = 1 \dots N$. Thus the solution of the random vector u involves computing the coefficients u_j in the polynomial representation from the known values of A_i and b_k . This is done by projecting (inner product) the above equation into each orthogonal basis function Φ_l leading to

$$A_i u_j \langle \Phi_i \Phi_j \Phi_k \rangle = b_k \langle \Phi_k \Phi_l \rangle \quad (4.3)$$

where the inner product is defined as follows

$$\langle x(\boldsymbol{\xi})y(\boldsymbol{\xi}) \rangle = \int_{\Theta} xyf(\boldsymbol{\xi})d\boldsymbol{\xi} \quad (4.4)$$

Using the orthogonality relation of the polynomials basis functions in Eq. 4.3 we get

$$A_i u_j \langle \Phi_i \Phi_j \Phi_k \rangle = b_k \langle \Phi_l^2 \rangle \delta_{lk} = b_l \langle \Phi_l^2 \rangle \quad (4.5)$$

Thus evaluation of the u_j 's involves solution of a coupled system. If the underlying deterministic system involves $ndof$ dequations, the coupled system involves $N \times ndof$ equations. Moreover, it needs explicit representations of the stochastic processes $a(\boldsymbol{\xi})$ and $b(\boldsymbol{\xi})$ in terms of the basis functions which may not be readily available and may involve more intrusive computations and change of the overall structure of the underlying deterministic code.

4.2 Decoupled system - NISG formulation

In the non-intrusive decoupled scheme, the output stochastic process is constructed using deterministic function evaluations at an optimal number of points defined in the input support space. Considering the linear system (Eq. (4.1)) again at specific points $\boldsymbol{\xi}_i$ of the support space we obtain

$$A(\boldsymbol{x}, \boldsymbol{\xi}_i)u(\boldsymbol{x}, \boldsymbol{\xi}_i) = b(\boldsymbol{x}, \boldsymbol{\xi}_i) \quad (4.6)$$

As can be observed, each function evaluation of A , u and b takes place at fixed points $\boldsymbol{\xi}_i$ in the random space. This can be equivalently expressed as

$$A_i(\boldsymbol{x})u_i(\boldsymbol{x}) = b_i(\boldsymbol{x}) \quad (4.7)$$

The above system can be solved for u_i at predetermined points of the support space which can be used to construct the solution $u(\boldsymbol{x}, \boldsymbol{\xi})$. The procedure is explained later in the section.

The specific function evaluation points are chosen from the consideration that in typical problems involving random variables, the quantities of interest are the probability density function, and the statistical moments of u . The p^{th} statistical moment can be calculated as follows:

$$M_p = \int_{\Theta} (u(\boldsymbol{x}, t, \boldsymbol{\xi}))^p f(\boldsymbol{\xi})d\boldsymbol{\xi} = \sum_{e=1}^{nel} \int_{\Theta_e} (u(\boldsymbol{x}, t, \boldsymbol{\xi}))^p f(\boldsymbol{\xi})d\boldsymbol{\xi} \quad (4.8)$$

where nel is the number of elements in the support space while Θ^e represents the local element domain. Using a Gauss quadrature integration scheme with n integration points per element, the above expression can be written as:

$$M_p = \sum_{e=1}^{nel} \sum_{i=1}^n w_i (u(\mathbf{x}, t, \boldsymbol{\xi}_i))^p f(\boldsymbol{\xi}_i) \quad (4.9)$$

where $\boldsymbol{\xi}_i$ denote the abscissae of the integration points while w_i denote the respective weights.

The above equation can be equivalently expressed as:

$$M_p = \sum_{e=1}^{nel} \sum_{i=1}^n w_i (u_i(\mathbf{x}, t))^p f(\boldsymbol{\xi}_i) \quad (4.10)$$

where $u_i(\mathbf{x}, t)$ denotes a deterministic space-time dependent process at each integration point of the support space.

Thus evaluation of u_i is completely deterministic and can be achieved using a readily available deterministic solution scheme and hence the non-intrusive terminology. To obtain the PDF of u denoted as $f_u(\boldsymbol{\xi})$, we first obtain the values of u at the nodal points of the discretized random space from the integration point values u_i . This can be achieved using a standard local or global least squares projection scheme. In this work we use a local least squares scheme. $f_u(\boldsymbol{\xi})$ can then be obtained by generating random monte-carlo samples from the PDFs of the input random variables $\boldsymbol{\xi}$, followed by evaluations of u at those points. It should be noted that this sampling does not require an explicit function evaluation but is generated from an interpolation of earlier evaluations using the appropriate interpolation order.

The developed scheme for discretization of the stochastic support space closely follows the finite element discretization of spatial domains in various applications and inherits all its properties. The the h and p convergence characteristics of the discretized domain are identical to the case of spatial finite elements. The error in this approximation is given by:

$$\begin{aligned} & \|u(x, t, \boldsymbol{\xi}) - u_{actual}(x, t, \boldsymbol{\xi})\|_{L_2(\Theta)} \quad (4.11) \\ & \leq \left(M \int_{\Theta} (u(x, t, \boldsymbol{\xi}) - u_{actual}(x, t, \boldsymbol{\xi}))^2 d\boldsymbol{\xi} \right)^{\frac{1}{2}} \leq M^{\frac{1}{2}} C(x, t) h^{q+1} \end{aligned}$$

where $M = \max_{\boldsymbol{\xi} \in \Theta} f(\boldsymbol{\xi})$, $C(x, t)$ is a deterministic function dependent on the nature of $u(x, t, \boldsymbol{\xi})$, q is the order of interpolation used to compute the PDF and h is the element size parameter.

The procedure for NISG analysis of large deformation processes can be summarized as follows.

- (1) Determine the PDF of the input uncertainties in terms of independent random variables $\{\xi_i\}_{i=1}^N$ and compute the joint PDF $f(\boldsymbol{\xi})$.
- (2) Determine the dimensionality of the support space. Based on the dimension discretize the support space using finite elements.
- (3) FOR $i=1$ to number of integration points
 - Compute the values of the random inputs at the support space integration point
 - Solve the deterministic large deformation problem with the given inputs and compute u_i - the output of interest.
 END
- (4) Compute u from the values of u_i using a global/local least squares interpolation.
- (5) Compute the moments as required from the u_i values as described in Eq. (4.9)

Thus, the NISG approach involves deterministic function evaluations at the integration points of the discretized support space of random variables which essentially translates to a decoupled approach for evaluating the additional degrees of freedom resulting from the randomness in the problem. The computational gains attained by this decoupling are significant. Also these gains can offset to a great extent the issue of slower convergence rate by the selection of a finer grid for the support space.

Remark 1. Though in this work we restrict ourselves to input random variables with uniform PDF's, the scheme can be extended to any other PDF whether bounded or unbounded by appropriately computing the joint PDF (Eq. (3.2)) and discretizing the support space. For input PDF's with unbounded support infinite domain elements can be used, as described in [17].

Remark 2. For support spaces with dimensionality less than 4, standard finite element grids can be used for domain discretization. To extend the approach to domains with dimensionality more than 3, tensor product finite element grids spaces to be considered.

4.3 Extension to full order reliability analysis

The state of art in reliability engineering consists of the First Order Reliability Method (FORM) and the Second Order Reliability Method (SORM) [18]. These methods were developed in the 70s and 80s when advanced stochastic analysis tools did not exist. These methods involve computing a first or a second order approximation of the limit state equation followed by calculation of the reliability index. The concept of reliability index which has been widely used and is still being used extensively was developed as a crude but conservative indicator of the failure probabilities. Using the above discussed non-intrusive analysis it is possible to get a full order estimate of the failure

probabilities without resorting to the concept of reliability index. To estimate the process failure probability we first define the limit state equation [18] which can be represented as a function of the stochastic process as follows:

$$Z = Z(u) = 0 \quad (4.12)$$

The probability of failure p_f (failure occurs when $Z \leq 0$) is given by

$$p_f = \int_{(Z < 0)} f_u(\boldsymbol{\xi}) d\boldsymbol{\xi} \quad (4.13)$$

Once $f_u(\boldsymbol{\xi})$ is obtained as discussed earlier, the above integral can be easily evaluated using a monte-carlo sampling approach leading to a direct evaluation of the failure probabilities without resorting to the calculation of the statistical moments or the reliability index.

5 Examples

We consider some applications of the proposed method in this section. Various sources of uncertainties are considered. The first problem examines the effect of uncertain friction and initial geometry on the force stroke characteristics. A reliability based design is also considered. The second application concerns with the effect of a random heterogeneous distribution of voids on the load displacement response of a tension specimen. The third application shows the effect of variation in the die shape on the material state of an extruded specimen. In all problems considered, the input uncertainties are assumed to have a uniform distribution. Also, first order (linear) elements are used to construct the support space in all examples leading to two integration points per random dimension in each element.

5.1 Problem 1 - Open die forging under random preform shape and random die-workpiece friction and reliability based design of forging press

We consider the benchmark problem of flat die upsetting of a cylinder here. Using symmetry only one-fourth of the domain is modelled. A power law constitutive model is employed here. The plastic flow function is taken as a power law model given by

$$f(\tilde{\sigma}, s, \theta) = \dot{\epsilon}_0 \left(\frac{\tilde{\sigma}}{s} \right)^n \quad (5.1)$$

where $\dot{\epsilon}_0 = 0.002 \text{ s}^{-1}$, $s = 150 \text{ MPa}$ and $n = 5$ while the elastic parameters are taken as $\lambda = 14423 \text{ MPa}$ and $\mu = 9615.4 \text{ MPa}$. A Gurson type damage

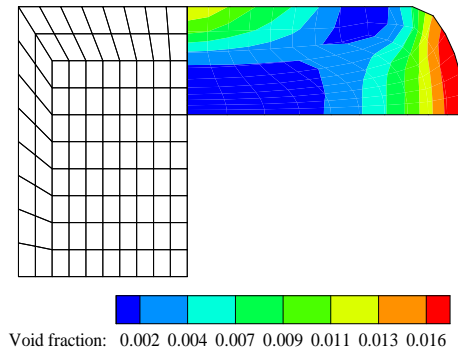


Fig. 2. Initial and final mean configurations for the cylinder upsetting process.

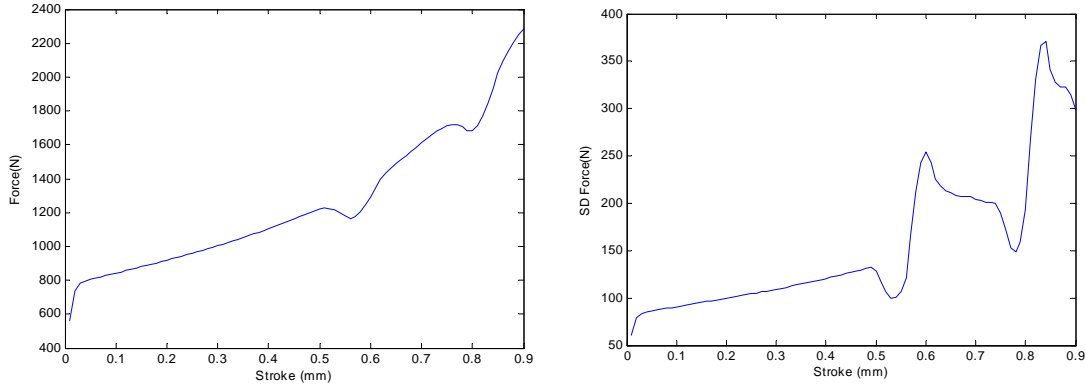


Fig. 3. Mean and standard deviation of the force vs stroke for the cylinder upsetting process.

evolution is also considered here. The details of the model are provided in [14]. An initial mean void fraction of 0.02 is assumed. The initial radius of the preform is assumed to vary uniformly between 0.9 and 1.1 mm while the die workpiece friction coefficient varies homogeneously between 0.1 and 0.5. The two random variables are assumed to be independent of each other. A 10×10 grid was used to represent the random support space leading to a total of 400 simulations. The initial height of the preform is 1.5 mm. The preform is subjected to a 60% height reduction. Fig. 2 shows the initial mean configurations and one of the realizations of the final mean configuration for the process while the statistics of the force vs stroke output are shown in Fig. 3. The standard deviation shows wide variations over the stroke length. Also the maximum value of the standard deviation is observed much before the point of the maximum value of the mean force giving an indication of the strong nonlinearities in the process. The comparisons of the statistics of final force value obtained using the proposed method with MC-LHS (Monte Carlo with Latin Hypercube Sampling) results are shown in Table 1. The MC-LHS convergence was only achieved after 20000 samples. As can be observed the results compare quite well with the work required being a fraction of that of the MC-LHS results in spite of substantial non-linearities due to foldover and contact. A similar problem was attempted in [2] using perturbation methods but the simulation was stopped before foldover occurred.

Table 1

Comparison of the statistics of the final load values for the cylinder upsetting process.

Parameter	MC-LHS (20000 samples)	10×10 uniform grid
<i>Mean</i>	2.2859e3	2.2863e6
<i>SD</i>	297.912	299.59
<i>m3</i>	-8.156e6	-9.545e6
<i>m4</i>	1.850e10	1.979e10

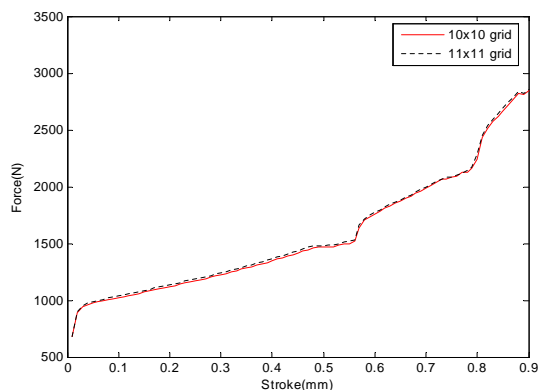


Fig. 4. Minimum required force capacity versus stroke plot for a press failure probability of 0.0002, corresponding to a reliability index of 3.54 for the cylinder upsetting process.

Reliability based design As seen in Fig. 3, the variations in the initial shape and the friction coefficient cause substantial difference in the maximum force requirement from the forging press. The objective here is to design the press for the process on the basis of the maximum force required based on a probability of failure of 0.0002. This would correspond to a reliability index of 3.54 for the case of standard normal variables. The failure probabilities for the whole process are plotted in Fig. 4. The maximum value of 2843 N occurs at the maximum stroke of .9 mm . To check the accuracy of results, a simulation using a 11x11 grid was also computed which gave a maximum of 2857 N at the same stroke. Thus the press needs to be designed to handle this force. Observe that the maximum force for the given failure probability does not occur at the maximum stroke.

5.2 Problem 2 - Effect of material heterogeneity on the response of a tension specimen.

This example shows the effect of random voids on the stochastic load-displacement response of a tension specimen. The material is assumed to have a random initial porosity derived from an assumed exponential correlation kernel using

Table 2

Comparison of the statistics of the final load values for the tension test

Parameter	MC-LHS (20000 samples)	6 × 6 uniform grid	7 × 7 uniform grid
<i>Mean</i>	6.1175	6.1176	6.1175
<i>SD</i>	0.799125	0.798706	0.799071
<i>M₃</i>	0.0831688	0.0811457	0.0831609
<i>M₄</i>	0.936212	0.924277	0.936017

a Karhunen Loève expansion [19] given by:

$$\mathcal{R}(\mathbf{p}_1, 0, \mathbf{p}_2, 0) = \sigma^2 \exp\left(\frac{-r}{b}\right) \quad (5.2)$$

where r is the distance between the points \mathbf{p}_1 and \mathbf{p}_2 , b is the correlation length assumed to be 5 mm and $\sigma = 0.5$. A truncated KL expansion sufficient to represent the heterogeneities for the stochastic void fraction using the above defined kernel can then be written as,

$$f(\mathbf{p}) = f_0 \left(1 + \sum_{i=1}^2 \xi_i \sqrt{\lambda_n} f_i(\mathbf{p})\right) \quad (5.3)$$

where $f_0 = 0.02$ is the assumed initial mean void fraction in the specimen. The random variables ξ_1 and ξ_2 assumed to be are uniformly distributed i.i.d variables. The damage evolution model is the same as in the previous example. The constitutive model employed here is for an 2024-T351 Al alloy at 300K. The isothermal version of the flow function is given by

$$f(\tilde{\sigma}, s, \theta) = \epsilon_0 \exp\left[\frac{1}{C} \left(\frac{\sigma}{s} - 1\right)\right] \quad (5.4)$$

and the state variable evolution is given by

$$s = A + B(\tilde{\epsilon}^p)^n \quad (5.5)$$

A 10×10 grid was used to model the random space. The initial configuration and the mean deformed configuration are shown in Fig. 5. The mean and standard deviation of the final void distribution are shown in Fig. 6. The mean and standard deviation of the load vs displacement curves are shown in Fig. 7. As can be observed random heterogeneities lead to substantial differences in the response of the specimen with variations observed in hardening and softening rates and onset of yielding. Also comparisons of the final force statistics obtained using our method and with 20000 MC-LHS samples are shown in Fig. 2 which are quite accurate.

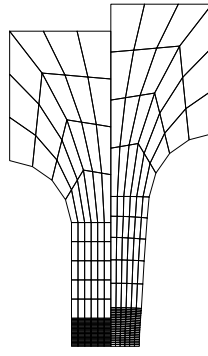


Fig. 5. Initial and final mean configurations for the tension test.

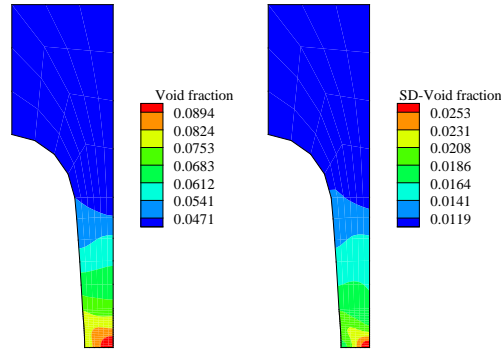


Fig. 6. Mean and standard deviation of the final void distribution for the tension test.

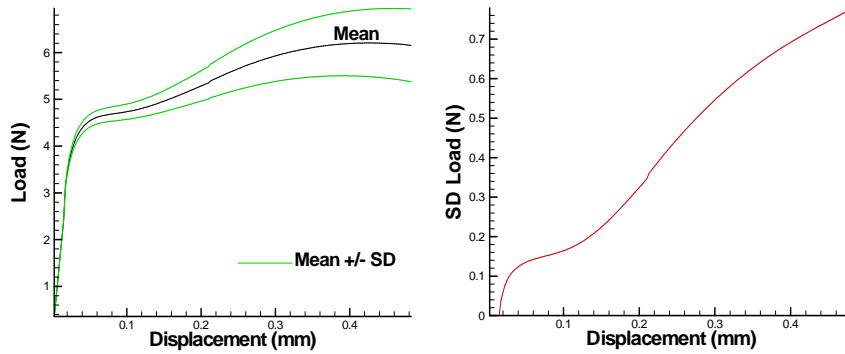


Fig. 7. Mean and standard deviation of the load displacement for the tension test.

5.3 Problem 3 - Stochastic estimation of die underfill caused by material porosity

This problem studies the effect of a random voids in the design of flashless closed die forging processes. The material is chosen to be an Fe-2% Si alloy at 1273 K with the material properties given in [14]. A hyperbolic sine flow function is assumed. The die-workpiece friction coefficient was taken as 0.1. For an initial billet with no voids having the same volume as the die (2.74mm^3), the deterministic flashless closed die forging process is shown in Fig. 8. The corresponding final state for the deterministic process with an initial void fraction of

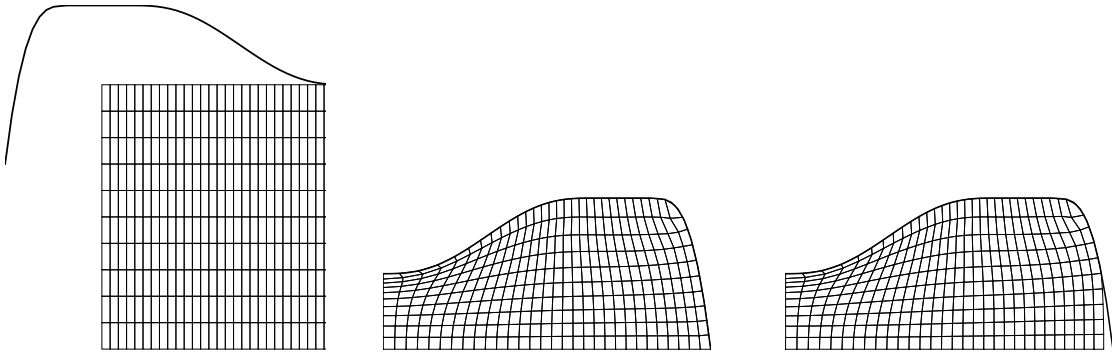


Fig. 8. Initial configuration (left), final configuration with no initial voids (center) final configuration an initial void fraction of 0.03 for the deterministic closed die forging simulation.

0.03 in the billet is also shown in the same figure. In the regions where there are compressive stresses, the void fraction decreases leading to a decrease in volume. The converse happens in regions of tensile stresses. As a result an underfill is observed in the process.

The NISG technique provides a robust way to estimate the statistics of the extent of die underfill as a result of a random distribution of voids in the billet. The initial void distribution is derived from an assumed exponential correlation kernel using a Karhunen Loéve expansion given by:

$$\mathcal{R}(\mathbf{p}_1, 0, \mathbf{p}_2, 0) = \sigma^2 \exp\left(\frac{-r}{b}\right) \quad (5.6)$$

where r is the distance between the points \mathbf{p}_1 and \mathbf{p}_2 , b is the correlation length assumed to be 5 mm and $\sigma = 0.1$. As in the earlier example, a truncated KL expansion sufficient to represent the heterogeneities for the stochastic void fraction can be written as,

$$f(\mathbf{p}) = f_0 \left(1 + \sum_{i=1}^2 \xi_i \sqrt{\lambda_n} f_i(\mathbf{p})\right) \quad (5.7)$$

where $f_0 = 0.03$ is the mean void fraction. A 9x9 grid was used for computing the statistics. The mean underfill was estimated to be $0.046976mm^3$ with a standard deviation of $0.0022mm^3$. Using a 10×10 support space grid the mean underfill was found to be $0.046187mm^3$ with a standard deviation of $0.0023mm^3$. The complete PDF of the underfill observed is plotted in Fig. 9

5.4 Problem 4 - Random material state in an extruded specimen driven by randomness in die geometry

In this example, we simulate an isothermal, extrusion operation with a die of average diameter reduction of 14%. The die geometry is given by,

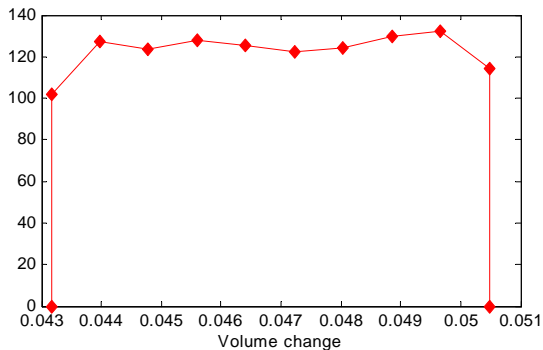


Fig. 9. Probability distribution of the underfill observed due to material porosity in the flashless closed die

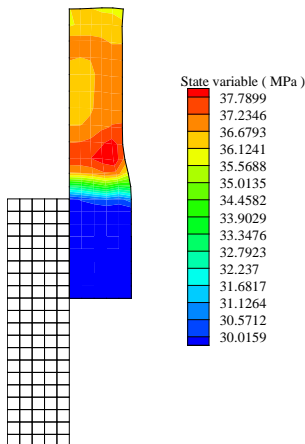


Fig. 10. Initial and final mean configurations for the isothermal extrusion problem.

$$z(\alpha) = 0.5\alpha \tag{5.8}$$

$$r(\alpha) = \sum_{i=1}^7 \beta_i \phi_i(\alpha)$$

For the deterministic problem we assume $\beta_1 = \beta_2 = \beta_3 = 0.5$, $\beta_4 = 0.46$, $\beta_5 = 0.44$, $\beta_6 = \beta_7 = 0.43$. The initial and final configurations for the deterministic simulation are shown in Fig. 10. The randomness is assumed in the parameters β_4 and β_5 given by $\beta_4 = 0.46(1 + 0.05\xi_1)$ and $\beta_5 = 0.44(1 + 0.05\xi_2)$, where ξ_1 and ξ_2 are uniformly distributed i.i.d variables. The objective of the problem is to ascertain the effect of uncertain die geometry on the steady state variable distribution at the exit. The simulation was observed to reach steady state after a time of 120s. A 9x9 grid is used to discretize the support space. The billet material is an Al 1100-O alloy at 673K with a hyperbolic sine flow function detailed in [20]. The die-workpiece friction coefficient was taken as 0.01. The mean and standard deviations of the state variable distribution at the die exit are plotted in Fig. 11. The figure shows that although the state variable values near the axis have a higher value, the standard deviation there is lower. As a comparison, the results obtained with a finer 10×10 grid are also plotted. It can be observed that there is very little difference between the statistics obtained using the two different discretizations.

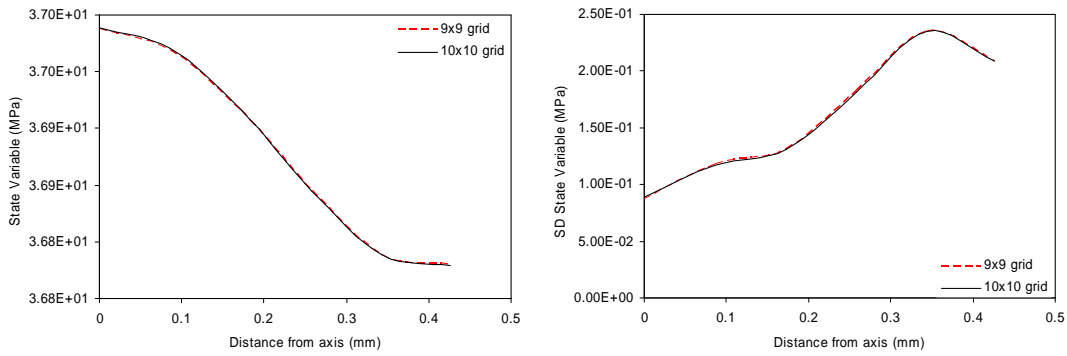


Fig. 11. Mean and standard deviation of the state variable at die exit.

6 Conclusions

This paper presented an efficient approach for non intrusive analysis of stochastic deformation processes. It was shown that this method can be easily implemented over legacy simulation softwares for deformation processes in both academia and industry with minimal effort, since the statistics are derived from deterministic simulations at the support space integration points. Example problems involving uncertainty in material properties and process conditions were considered showing effectiveness of this method in predicting uncertainty propagation in deformation processes. The method showed excellent comparisons with the Monte-Carlo method for the first two examples. An example considering reliability based design was also demonstrated.

Though this method provides an attractive alternative compared to the intrusive techniques, it does suffer from the curse of dimensionality and is not suitable for problems involving high dimensional uncertainties in its present form. Methods such as h and p adaptive discretization of the support space, sparse grid and dimension adaptive quadrature techniques [21] can significantly reduce the curse of dimensionality. Some of these issues are being actively addressed and will form the basis of a future publication.

7 Acknowledgements

The work presented here was funded by the Computational Mathematics program of the Air Force Office of Scientific Research (grant F49620-00-1-0373). Additional support was provided by the Engineering Design Division of DMI of the National Science Foundation (grant DMI-0113295). The computing for this project was supported by the Cornell Theory Center, which receives funding from Cornell University, New York State, federal agencies, and corporate partners.

References

- [1] I. Doltsinis, Inelastic deformation processes with random parameters methods of analysis and design, *Computer Methods in Applied Mechanics and Engineering* 192 (2003) 2405–2423.
- [2] I. Doltsinis, Perturbation-based stochastic FE analysis and robust design of inelastic deformation processes, *Computer Methods in Applied Mechanics and Engineering*, in press.
- [3] M. Grzywinski, A. Sluzalec, Stochastic equations of rigid-thermo-viscoplasticity in metal forming process, *International Journal of Engineering Science* 40(2002) 367–383.
- [4] A. Sluzalec, Simulation of stochastic metal-forming process for rigid-viscoplastic material, *International Journal of Mechanical Sciences* 42 (2000) 1935–1946.
- [5] M. Kleiber, J. Knabel, J. Rojek, Response surface method for probabilistic assessment of metal forming failures, *International Journal for Numerical Methods in Engineering* 60 (2004) 51–67.
- [6] D. Xiu, G. E. Karniadakis, The Wiener -Askey polynomial chaos for stochastic differential equations , *Siam J. Sci. Comput.* 24 (2002) 619-644.
- [7] S. Acharjee, N. Zabarar, Uncertainty propagation in finite deformations A spectral stochastic Lagrangian approach, *Computer Methods in Applied Mechanics and Engineering*, in press.
- [8] M. A. Tatang, W. W. Pan, R. G. Prinn, and G. J. McRae, An efficient method for parametric uncertainty analysis of numerical geophysical model, *Journal of Geophysical Research-Atmospheres*, D18 (1997) 21925–21932.
- [9] L. Mathelin, M. Y. Hussaini, T. A. Zang and F. Bataille, Uncertainty propagation for turbulent compressible flow in quasi-1d nozzle using stochastic collocation method, *Proceedings of the 16th AIAA Computational Fluid Dynamics Conference* June 2326, 2003/Orlando, Florida.
- [10] M. T. Reagan, H. N. Najm, R. G. Ghanem, O. M. Knio, Uncertainty quantification in reacting-flow simulations through non-intrusive spectral projection, *Combust. Flame* 132 (2003) 545–555.
- [11] M. K. Deb, I. M. Babuska and J. T. Oden, Solution of stochastic partial differential equations using Galerkin finite element techniques, *Comp. Meth. Appl. Mech. Engrg.* 190 (2001) 6259–6372.
- [12] N. Zabarar, S. Ganapathysubramanian, Q. Li, A continuum sensitivity method for the design of multi-stage metal forming processes, *Int. J. Mech. Sciences* 45 (2003) 325–358.
- [13] S. Ganapathysubramanian, N. Zabarar, A continuum sensitivity method for finite thermo-inelastic deformations with applications to the design of hot forming processes, *Int. J. Numer. Methods Engrg.* 55 (2002) 1391–1437.

- [14] A. Srikanth, N. Zabararas, A computational model for the finite element analysis of thermoplasticity with ductile damage at finite strains, *International Journal for Numerical Methods in Engineering* 45 (1999) 1569–1605.
- [15] R. V. Field Jr., M. Grigoriu, On the accuracy of the polynomial chaos approximation, *Probabilistic Engineering Mechanics* 19 (2004) 65–80.
- [16] B. N. Velamuri Asokan, N. Zabararas, Using stochastic analysis to capture unstable equilibrium in natural convection, *Journal of Computational Physics* 208 (2005) 134-153.
- [17] O. C. Zienkiewicz, and R. L. Taylor *The Finite Element Method: Volume 1, The Basics*, Butterworth-Heinemann, 2000.
- [18] A. Haldar, S. Mahadevan, *Reliability assessment using stochastic finite element analysis*, John Wiley and Sons, Inc., New York, 2000.
- [19] R. Ghanem, P.D. Spanos, *Stochastic finite elements: A spectral approach*, Springer-Verlag, New York, 1999.
- [20] S.B. Brown, K.H. Kim, L. Anand, An internal variable constitutive model for hot working of metals, *International Journal of Plasticity* 5 (1989) 95-130.
- [21] A. Keese, H. G. Matthies, *Numerical Methods and Smolyak Quadrature for Nonlinear Stochastic Partial Differential Equations*, Technical report, Institute of Scientific Computing, Technical University Braunschweig Brunswick, Germany, 2003.